Chinese Chemical Letters 36 (2025) 110228

Contents lists available at ScienceDirect

Chinese Chemical Letters

journal homepage: www.elsevier.com/locate/cclet

Systemically intravenous siRNA delivery into brain with a targeting and efficient polypeptide carrier and its evaluation on anti-glioma efficacy

Liqing Chen[a,b,1], Zheming Zhang[a,b,1], Yanhong Liu[a,b], Chenfei Liu[a,b], Congcong Xiao[a,b], Liming Gong[a,b], Mingji Jin[a,b], Zhonggao Gao[a,b,*], Wei Huang[a,b,*]

[a] State Key Laboratory of Bioactive Substance and Function of Natural Medicines, Institute of Materia Medica, Chinese Academy of Medical Sciences and Peking Union Medical College, Beijing 100050, China
[b] Beijing Key Laboratory of Drug Delivery Technology and Novel Formulations, Department of Pharmaceutics, Institute of Materia Medica, Chinese Academy of Medical Sciences and Peking Union Medical College, Beijing 100050, China

ARTICLE INFO

Article history:
Received 21 April 2024
Revised 30 June 2024
Accepted 8 July 2024
Available online 8 July 2024

Keywords:
15-Amino-acid peptide
Glioma
Brain targeting
Gene silencing
Transvascular delivery

ABSTRACT

Gliomas are the most common intracranial tumors with poor survival and high mortality. Furthermore, the clinical efficacy of current drugs is still not ideal; despite the development of several therapeutic drugs over the past decades and tumor progression or recurrence is inevitable in many patients. RNAi-based therapy presents a novel disease-related gene targeting therapy, including otherwise undruggable genes, and generates therapeutic options. However, the therapeutic effect of siRNA is hindered by multiple biological barriers, primarily the blood-brain barrier (BBB). A glycoprotein-derived peptide-mediated delivery system is the preferred option to resolve this phenomenon. RDP, a polypeptide composed of 15 amino acids derived from rabies virus glycoprotein (RVG), possesses an N-type acetylcholine receptor (nAChR)-binding efficiency similar to that of RVG29. Given its lower cost and small particle size when used as a ligand, RDP should be extensively evaluated. First, we verified the brain-targeting efficacyy of RDP at the cellular and animal levels and further explored the possibility of using the RDP-oligoarginine peptide (designated RDP-5R) as a bio-safe vehicle to deliver therapeutic siRNA into glioma cells *in vitro* and *in vivo*. The polypeptide carrier possesses a diblock design composed of oligoarginine for binding siRNA through electrostatic interactions and RDP for cascade BBB- and glioma cell-targeting. The results indicated that RDP-R5/siRNA nanoparticles exhibited stable and suitable physicochemical properties for *in vivo* application, desirable glioma-targeting effects, and therapeutic efficiency. As a novel and efficient polypeptide carrier, RDP-based polypeptides hold great promise as a noninvasive, safe, and efficient treatment for various brain diseases.

Gliomas account for approximately 30% of central nervous system (CNS) tumors and 80% of malignant brain tumors [1,2]. Despite the application of aggressive multimodality approaches, tumor progression or recurrence is inevitable in many patients. The median survival of patients with glioblastoma (GBM) is less than 15 months, and the five-year survival rate is estimated at 5% [3]. Major therapeutic obstacles include the invasive properties of the tumor cells, tumor cell resistance to chemotherapy, poor penetration across the blood-brain barrier (BBB), and suboptimal tumor penetration [4]; therefore, few drugs have been approved by the Food and Drug Administration (FDA) for the treatment of glioma. Despite the development of cancer therapies over the past decades, the clinical efficacy of the current drugs is still not ideal.

In recent years, RNA interference (RNAi)-based therapies have emerged as potential gene-targeted treatments for various brain-related diseases. With rational sequence design, small interfering RNA (siRNA) can be exploited to down-regulate (or silence) the expression of disease-related genes, including otherwise undruggable genes with high efficiency, enlarging therapeutic options. Among them, the survivin gene is frequently used as a target gene for RNAi. As a member of the inhibitor of apoptosis (IAP) gene family. survivin proteins have been proven to inhibit apoptosis, regulate the cell cycle, and promote cell proliferation and angiogenesis. Survivin is primarily found in small amounts in embryos and some immaturely differentiated normal human tissues [5] and is

* Corresponding authors.
E-mail addresses: zggao@imm.ac.cn (Z. Gao), huangwei@imm.ac.cn (W. Huang).
[1] These authors contributed equally to this work.

https://doi.org/10.1016/j.cclet.2024.110228
1001-8417/

not expressed in other differentiated and mature tissues [6], but is highly expressed in most tumors and exhibits overexpression at different stages of tumor development [7]. Nevertheless, effective and safe systemic delivery of siRNA into the brain is severely hindered by multiple biological barriers, such as short circulation lifetime, BBB, suboptimal tissue penetration, cell endocytosis, and intracellular transport [8]. Nanotechnology offers intriguing potential to resolve these challenges in siRNA delivery. Among the non-viral vectors, cationic lipids and polymers are the most extensively studied. However, the transfection efficiency of these lipids and polymers into neuronal cells is lower than in other mammalian cells due to their reduced mitotic activity [9-11]. The treatment of brain tumors needs to consider the toxicity posed by nanocarriers to normal neuronal cells. Considering the particularity and significance of the physiological structure of the brain, developing biodegradable, biocompatible, and bio-safe nanocarriers for intravenous siRNA delivery is essential and meets the clinical requirements of glioma treatment. However, concerning transfection efficiency and toxicity, siRNA delivery to the CNS by polyplexes or lipoplexes is still unsatisfactory.

New brain-targeting peptides have been developed to achieve nanoparticle-mediated targeted drug delivery for glioma treatment. Some display a bifunctional role, simultaneously mediating BBB penetration and enhancing glioma cell endocytosis, such as peptide T7, angiopep-2 [12-16]. The rabies virus glycoprotein (RVG)-derived peptide with a 29-amino acid sequence (RVG29) specifically binds N-type acetylcholine receptor (nAChR) on the surface of nerve cells in the BBB and glioma cells with high nAChR expression, but not nAchR-negative cells, and mediate the entry of drugs across the BBB and glioma cells [17,18]. As a well-known member of brain-targeted ligands, RVG29 has been employed as a ligand for efficient nucleic acids and small molecular chemicals delivery into the brain to diagnose and treat various brain diseases, such as glioma, Alzheimer's disease, Parkinson's disease, ischemic injury, protein misfolding diseases [19-24]. Moreover, a RVG29-conjugated cationic oligopeptide has been used to successfully transport siRNA across the BBB to neuronal cells in the CNS by intravenous administration, and repeated administration did not induce inflammatory cytokines or anti-peptide antibodies [17].

Given that the length of RVG29, cost and particle size of nanocarriers using RVG29 as ligands are dissatisfactory. In particular, large particles penetrate the tumor parenchyma less effectively. RDP, with only 15 amino acids, is expected to display more beneficial potentials in the treatment of brain diseases. In this study, we first verified the brain-targeting efficiency of RDP at the cellular and animal levels. Furthermore, we explored the possibility of using an RDP-oligoarginine peptide (designated RDP-5R) as a novel and efficient vehicle to deliver therapeutic siSur into glioma cells *in vitro* and *in vivo*. Ultimately, we found that not all targeting peptide-oligoarginine polypeptide carriers can self-assemble to encapsulate siRNA in our previous work, considering the different water solubility and spatial potential resistance of different targeting peptides. In this study, the designed polypeptide has a diblock design composed of oligoarginine for binding siRNA through electrostatic interactions and RDP for cascade BBB and glioma targeting based on a single ligand [25]. In this drug delivery system, RDP mediates efficient BBB and glioma targeting *in vitro* and *in vivo* and possesses improved application performance than the RVG29. RDP-R5/siSur nanoparticles (NPs) demonstrate superior physicochemical properties, enhanced siRNA uptake, gene silencing efficacy, apoptosis induction, S phase arrest, and inhibitory effects on glioma cell growth and metastasis *in vitro*. Notably, RDP-R5/siSur NPs simultaneously suppress orthotopic glioma growth and spontaneous metastasis to the liver or lungs in an orthotopic glioma model, thereby prolonging the survival rate. In this study, the polypeptide RV-MAT, homologous to RVG29 but without binding activity, has been used as the scrambled peptide when necessary in the whole study [17].

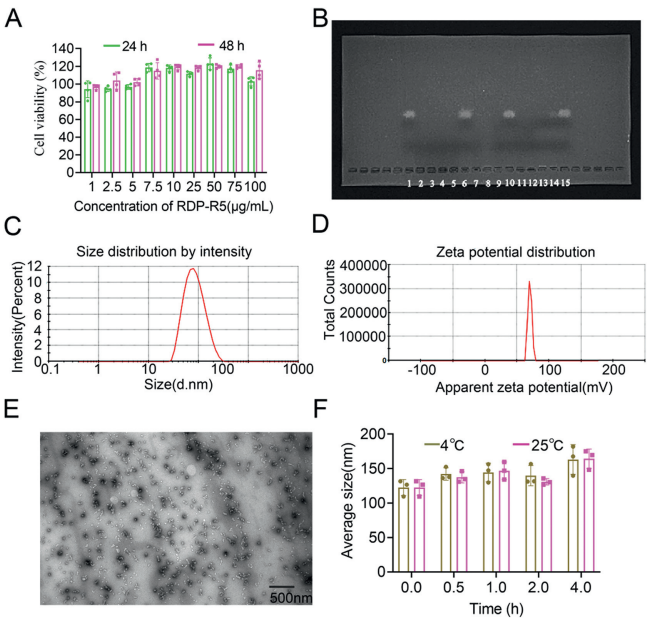

Fig. 1. (A) Cell viability of C6-Luc cells incubated with different concentrations of RDP-R5 for 24 or 48 h ($n = 3$). (B) Gel retardation assay of RDP-R5/siRNA NPs prepared at different N/P ratios (1, 6, 10, 15: naked siRNA; 2: N/P = 500:1; 3: N/P = 400:1; 4: N/P = 300:1; 5: N/P = 200:1; 7: N/P = 100:1; 8: N/P = 50:1; 9: N/P = 20:1; 11: N/P = 10:1; 12: N/P = 5:1; 13: N/P = 2:1; 14: N/P = 1:1). (C) Size distribution of RDP-R5/siRNA NPs (N/P = 50:1). (D) Zeta-potential of RDP-R5/siRNA NPs (N/P = 50:1). (E) TEM image of RDP-R5/siRNA NPs (N/P = 50:1). (F) Size stability of RDP-R5/siRNA NPs after being placed at 4 or 25 °C respectively ($n = 3$, N/P = 50:1). Data are presented as mean ± standard deviation (SD).

It is worth mentioning that RDP-R5 as a nucleic acid delivery vector has been applied for a Chinese invention patent by our lab and has recently been authorized (ZL201810317197.X). As a fragment of RVG29, RDP has the same alpha-subunit binding active sequence, RVG189-199, and is proposed to possess a similar neural affinity. In this study, the specific binding of RVG15 to neurocytes was investigated for the first time. Neuro-2a and C6 cells were used as model cell lines due to their abundant nAchR expression [26,27]. Neuro-2a and C6 cells demonstrated strong fluorescence intensity and significant RDP uptake; however, three kinds of peripheral cells demonstrated less RDP uptake under fluorescence microscopy (Fig. S1A in Supporting information), suggesting that RDP possess a good selective binding to neurons overexpressing nAchR. The inverted fluorescence microscope and flow cytometer (FCM) analyses were conducted to compare the brain-targeting activity of RDP and RVG29. As presented in Fig. S1B (Supporting information), the uptake of RDP and RVG29 by Neuro-2a cells was similar under an inverted fluorescence microscope. Furthermore, this phenomenon was consistent with the FCM analysis (Figs. S1C and D in Supporting information), and RDP uptake was slightly lower than that of RVG29 in Neuro-2a cells; however, the difference was insignificant. The above results imply that RDP exhibits a similar brain-targeting ability to RVG29 and holds great promise as a substitute for RVG29 in practice.

As presented in Fig. 1A, the viability of C6-Luc cells incubated with 1–100 μg/mL RDP-R5 for 24 or 48 h was above 90%, suggesting that RDP-R5 was a relatively safe siRNA delivery vector with almost no cytotoxicity. A gel electrophoresis assay was performed to investigate the shrinkage ability of RDP-R5 for siRNA at different N/P ratios ranging from 1:1 to 500:1. The gel imaging results (Fig. 1B) revealed no free siRNA stripe at any N/P ratio, implying that RDP-R5 condensed siRNA efficiently when the N/P ratio was

above 1:1. Figs. 1C–E indicate that RDP-R5/siRNA NPs (N/P: 50/1) had an average particle size of (74.46 ± 3.50) nm, polydispersity index (PDI) of 0.210 ± 0.01, and zeta potential of (20.6 ± 1.2) mV, with a spherical structure, smooth surface and uniform distribution. The results indicated that the RDP-R5/siRNA-NPs were small, uniform, and positively charged. Simultaneously, RVG29-R5/siRNA NPs were prepared in the same process. As presented in Table S1 (Supporting information), RVG29-R5/siRNA NPs had a particle size of (122.07 ± 2.95) nm, PDI of 0.190 ± 0.02, and zeta potential of (22.5 ± 1.8) mV. Compared with RVG29-R5/siRNA NPs, RDP-R5/siRNA NPs had relatively smaller and more uniform particle sizes. Reducing the length of the amino acid sequence by half reduced the production cost and the particle size, implying that RDP-R5 is superior as a target ligand for brain-targeted delivery. The stability of the RDP-R5/siRNA-NPs at 4 °C and room temperature (RT) was investigated. As presented in Fig. 1F, the particle size of the NPs did not change significantly within 2 h; however, it increased after 4 h either at 4 °C or RT, which indicated that a short storage time (≤2 h) at RT had no significant effect on the size stability of NPs. Furthermore, the serum stability of RDP-R5/siRNA NPs was evaluated the agarose gel electrophoresis analysis [17,28,29]. The results (Fig. S2 in Supporting information) showed that most siRNA was still stuck in the well even at 24 h, suggesting the relative long-term stability of RDP-R5/siRNA NPs *in vivo*. The RiboGreen (Thermo Fisher, MA) assay was used for the encapsulation efficiency (EE) assay. Ribogreen is an embedded fluorescent dye of double-stranded RNA, which can be used for quantitatively detecting pg-level RNA; however, it is well suited for determining siRNA in non-viral vectors. In addition, the method was validated by assessing the linear relationship, precision, recovery, and sample stability, which suggested that this method was suitable for the accurate quantitation of siRNA. The EE of RDP-R5/siRNA NPs calculated was 96.61% ± 2.04%.

Successful application of NPs for therapeutic purposes requires their effective uptake by cells. There is extensive experimental evidence that the physicochemical characteristics of NPs, biological medium, and cell status affect the uptake of NPs in cells [30]. Herein, we examined factors affecting glioma cell uptake of RDP-R5/siRNA NPs to obtain suitable transfection conditions for subsequent experiments. The results indicated that the uptake efficiency of RDP-R5/siFAM NPs depended on incubation time, siRNA dosage, and transfection medium. Cellular uptake efficiency was improved with an increase in transfection time (Fig. S3A in Supporting information) and siRNA dosage (Fig. S3C in Supporting information) and decreased significantly in 20% FBS and 10% FBS medium compared to 0% FBS medium ($^{***}P < 0.001$ and $^{**}P < 0.01$, respectively) (Fig. S3B in Supporting information). Based on the above results, the uptake efficiency of the different formulations was further investigated under 40 nmol/L transfection dosage, incubation for 2 h, and serum-free transfection medium. As presented in Fig. S4A (Supporting information), no significant siFAM were uptaken by C6-Luc cells in the naked siFAM group and RV-MAT-R5/siFAM group; however, cells incubated with RDP-R5/siFAM NPs demonstrated high fluorescence intensity. Similar results were obtained using the FCM analysis. There was no significant difference in the fluorescence intensity between the two negative control groups (naked siFAM and RV-MAT-R5/siFAM) and the blank control group. Nevertheless, the fluorescence intensity of the RDP-R5/siFAM group was significantly higher than those of the naked siFAM and RV-MAT-R5/siFAM groups ($^{***}P < 0.001$, Fig. S4B in Supporting information). In summary, RDP-R5 enabled the effective delivery of siRNA into glioma cells.

Moreover, the effect of incubation time and transfection medium on gene reporter silencing efficiency (Figs. 2A and C) was in line with the cellular uptake efficiency. In addition, the N/P ratio is a crucial factor affecting gene silencing efficiency, given that the

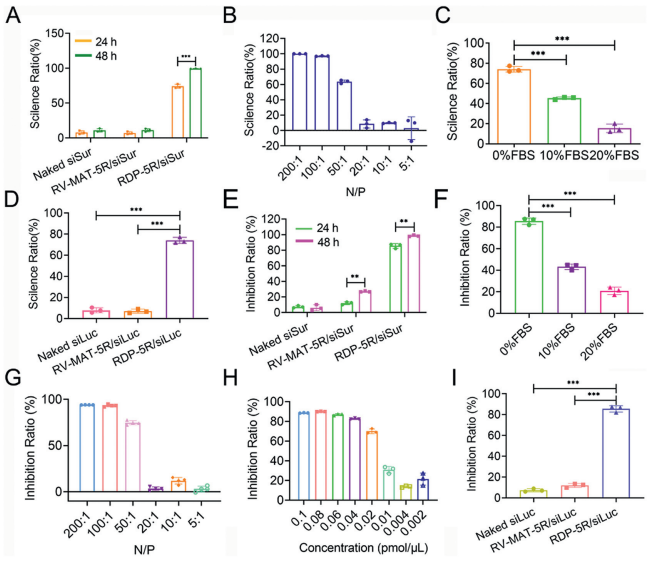

Fig. 2. *In vitro* gene silence and antitumor effect of RDP-R5/siRNA NPs. (A) Luciferase gene silence efficiency of RDP-R5/siLuc on C6-Luc cells incubated at different time, (B) N/P ratios, (C) transfection medium ($n = 3$), and (D) gene silence efficiency of different formulations ($n = 3$). (E) Cell proliferation inhibition ratio of RDP-R5/siSur NPs on C6-Luc cells at different times, (F) transfection medium, (G) N/P ratios ($n = 4$), (H) siSur concentration ($n = 3$), and (I) inhibition ratio of different formulations ($n = 3$). $^{**}P < 0.01$, $^{***}P < 0.001$. RV-MAT: scrambled peptide. Data are presented as mean ± SD.

size and surface potential of NPs is related to the N/P ratio. When the N/P ratio was above 50:1, the gene-silencing efficiency of RDP-R5/siLuc NPs was markedly elevated (Fig. 2B). The gene silencing efficiency of different formulations was investigated with an N/P ratio of 50:1, a dosage of 40 nmol/L, and a serum-free medium for 24 h. As presented in Fig. 2D, the average silencing efficiency of the endogenous luciferase gene by RDP-R5/siLuc NPs was 74.06%, significantly higher than that of the naked siLuc group (7.88%) and the RV-MAT-R5/siLuc NPs group (6.99%) ($^{***}P < 0.001$). The results indicated that RDP-R5/siLuc NPs could successfully deliver siRNA into cells and effectively silence target genes. As shown in Fig. S5 (Supporting information), when given 80 nmol/L of RVG29-R5/siNC NPs, the uptake amount of RDP-R5/siCy5 NPs by C6 cells was significantly reduced, indicating that the binding sites of RDP is identical to RVG29.

Subsequently, the cell proliferation inhibition ratio of the RDP-R5/siSur NPs was assessed using the cell counting kit-8 (CCK-8) assay. Consistent with the reporter gene silencing assay, the inhibition ratio of RDP-R5/siSur NPs depended on the incubation time, N/P ratios, and transfection medium (Figs. 2E–G). Furthermore, RDP-R5/siSur NPs inhibited the proliferation of C6-Luc cells in a concentration-dependent manner (Fig. 2H). In addition, the inhibition ratio of different formulations was investigated at an N/P ratio of 50:1, a dosage of 40 nmol/L, and serum-free medium for 24 h. Fig. 2I reveals that the inhibition ratio of RDP-R5/siSur NPs on the proliferation of C6-Luc cells was 85.54% and was significantly higher than that of naked siSur (7.36%) and RV-MAT-R5/siSur NPs (11.54%) ($^{***}P < 0.001$), indicating that RDP-R5/siSur NPs effectively inhibited the proliferation of glioma cells.

Meanwhile, Western blot (WB) was used to analyze the expression of survivin protein in cells treated with RDP-R5/siSur NPs. As shown in Fig. 3A, the RDP-R5/siSur NPs group had the lowest amount of survivin protein among the four tested formulations and RV-MAT-R5/siSur groups also showed reduced survivin protein expression. Almost no reduction of survivin protein expression in the naked siSur group. These results were similar to the densitometry quantification for WB (Fig. 3B). The survivin protein in RDP-

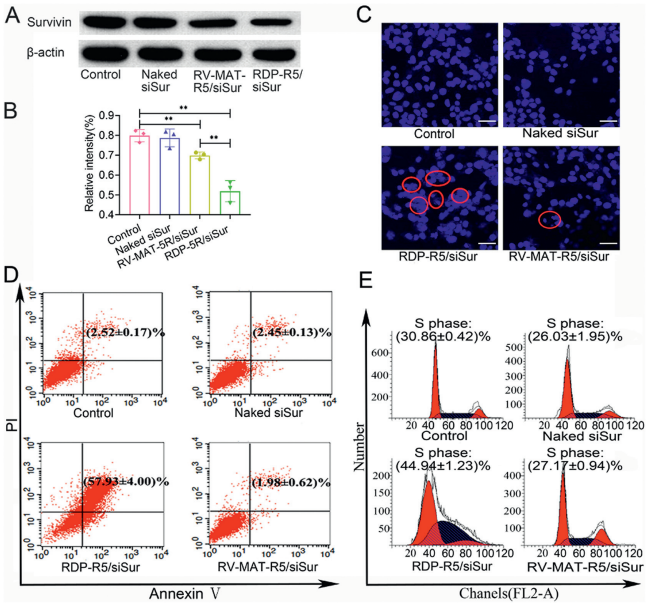

Fig. 3. (A) Representative WB images for survivin proteins detection of cells incubated with different formulations. (B) Densitometry quantification for WB images ($n = 3$). $^{**}P < 0.01$. (C) The inverted fluorescent microscope images of C6-Luc cells incubated with different formulations (red cycles indicate apoptotic cells), magnification 200×. Scale bar: 50 μm. (D) FCM results of Annexin V-FITC/PI double staining assay of different groups. (E) Cell cycle arrest induced by different formulations. Data are presented as mean ± SD.

R5/siSur NPs decreased significantly compared to the control and RV-MAT-R5/siSur groups ($^{**}P < 0.01$).

In addition, a large area of nuclear shrinkage and fragmentation (red cycles) was observed in C6-Luc cells treated with RDP-R5/siSur NPs for 24 h, indicating that glioma cells were highly apoptotic. In addition, some cells in the RV-MAT-R5/siSur NPs group demonstrated nuclear fragmentation, and the degree of apoptosis was slight; however, no apoptosis occurred in the naked siSur group (Fig. 3C). Annexin V-fluorescein isothiocyanate (FITC)/propidium iodide (PI) double staining was adopted to measure the apoptosis of C6-Luc cells using flow cytometry quantitatively. The results of FCM analysis indicated that the proportion of apoptotic cells (Annexin-FITC$^+$/PI$^-$ and Annexin-FITC$^+$/PI$^+$) treated with RDP-R5/siSur NPs increased compared to naked siSur and RV-MAT-R5/siSur groups (Fig. 3D). The proportion of late apoptotic cells reached 57.93% ± 4.00%, which was significantly higher than that of the two negative control groups ($^{***}P < 0.001$). These results implied that RDP-R5/siSur NPs demonstrated a stronger ability to induce apoptosis, which was consistent with the experimental results of the CCK-8 assay. Fig. 3E indicates that C6-Luc cells could be blocked in the S phase after 24 h of transfection with RDP-R5/siSur NPs. There was no significant difference between the negative control (naked siSur and RV-MAT-R5/siSur NPs) and the blank control group.

The metastatic nature of brain tumor cells contributes to the ineffectiveness of current treatment modalities. Glioma cells, especially GBM, can invade the surrounding normal brain tissues, making complete resection of tumors impossible and easy to recur after treatment [31]. Therefore, suppressing glioma metastasis is crucial for improving prognosis and long-term survival. The inhibitory effect of RDP-R5/siSur NPs on the transverse migration of glioma cells was investigated using a cell wound healing assay. As presented in Figs. S6A and B (Supporting information), the scratches in the blank control group and the two negative control groups healed gradually. In contrast, the scratches remained visible when treated with RDP-R5/siSur NPs, and cell density near the scratch decreased, accompanied by many apoptotic or dead cells and irregular cell morphology. The results indicated that RDP-R5/siSur NPs have significant inhibitory effect on the viability and migration of glioma cells, suggesting that RDP-R5/siSur exerts anti-metastatic effects on glioma cells.

The BBB consists mainly of human brain microvascular endothelial cells (HBMECs), astrocytes, and pericytes. Due to the selective permeability, it is difficult for drugs to permeate the central lesion through the BBB. Tumors are known to compromise the integrity of the BBB [32]. However, BBB and the blood-brain tumor barrier (BBTB) restrict the passage of most drugs into the brain and tumors [33], especially in tumor infiltration areas and tumor neovascularization. Therefore, it is necessary to investigate the ability of these drugs to penetrate the BBB. Herein, we first verified the cytotoxicity of RDP-R5 on HBMECs at concentrations 1–100 μg/mL. Considering each group's 90% cell viability (Fig. S7A in Supporting information), RDP-R5 is a relatively safe brain-targeted delivery carrier and can deliver siRNA without damaging the BBB. After establishing the BBB model *in vitro* as illustrated, transendothelial electrical resistance (TEER) values and sodium fluorescein permeability tests were conducted to investigate the integrity and barrier function of the BBB model. On the 11th day post-incubation, TEER reached $(258 \pm 12.16)\ \Omega\ cm^2$ and the permeability coefficient of sodium fluorescein was 10.67×10^{-6} cm/s, similar to a previous report in which the coefficient was about $(11 \pm 1.5) \times 10^{-6}$ cm/s [34], confirming that HBMEC layers were confluent and reliable for transport assays. As presented in Fig. S7B (Supporting information), the Papp value of RDP-R5/siRNA NPs increased continuously within 120 min; however, the Papp of two negative control groups, naked siRNA and RV-MAT-R5/siRNA NPs, increased slowly and was lower than that of RDP-R5/siRNA NPs at 120 min. The Papp value of RDP-R5/siRNA NPs reached 281.48×10^{-6} cm/s at 120 min, which was 2.1 times higher than that of the RV-MAT-R5/siRNA NPs group ($^{***}P < 0.001$) and 1.96 times higher than that of the naked siRNA NPs group ($^{***}P < 0.001$), indicating that RDP-R5 endowed siRNA with BBB traversing potential. As seen in Figs. S7C and D (Supporting information), HBMEC had obvious uptake of RDP-R5/siFAM NPs, significantly higher than the other groups ($^{***}P < 0.001$). The high BBB traversing potential of RDP-R5/siFAM NPs may be attributed to adequate internalization and intracellular transport of siRNA by nAChR-mediated endocytosis.

With siCy5 as a tracer, real-time *in vivo* fluorescence imaging was used to investigate the targeting ability of RDP-R5/siCy5 NPs in C6-Luc tumor-bearing mice and non-tumor-bearing mice. All animal experiments were ethically approved by the Laboratory Animal Ethics Committee of the Institute of Materia Medica, Chinese Academy of Medical Sciences and Peking Union Medical College. All operational procedures adhered to the national and institutional principles and protocols for treating experimental animals.

For tumor-bearing mice, after 1 h of administration, no significant fluorescence was detected in the naked siCy5 group because of the fast siRNA damage and excretion in the circulation system. Furthermore, suboptimal amounts of RV-MAT-R5/siCy5 NPs accumulated in the brain area due to their low BBB permeation and poor cellular uptake. In contrast, RDP-R5/siCy5 NPs had the highest fluorescence intensity in the brains of tumor-bearing mice (Fig. S8A in Supporting information), which indicated that RDP-R5/siCy5 NPs possess superior brain-targeting ability after intravenous injection as a result of nAChR-mediated transcytosis. Next, mice were sacrificed 1 h post-administration to observe the accumulation of siRNA in the major organs. The heart, liver, spleen, lung, kidney, and brain were dissected and subjected to real-time *in vivo* fluorescence imaging. These results were consistent with *in vivo* fluorescence imaging. Higher fluorescence intensity was observed at the tumor site in the brain of the RDP-R5/siCy5 group, while almost no fluorescence was observed in the brain of the naked siCy5

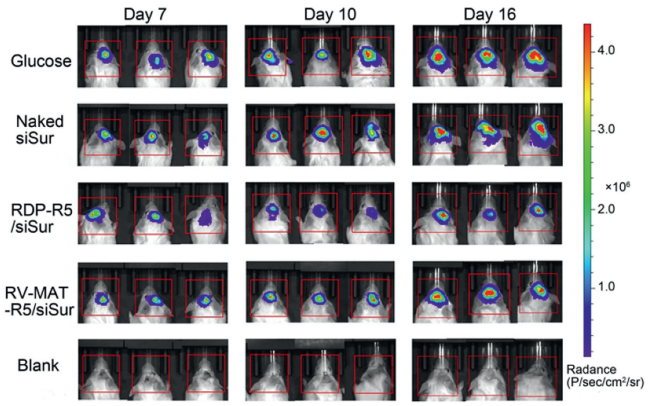

Fig. 4. *In vivo* bioluminescence images of orthotopic glioma bearing mice treated with glucose, naked siSur, RDP-R5/siSur and RV-MAT-R5/siSur *via* tail vein injection (siSur: 1.5 mg/kg) at different time points, and blank group was injected with normal saline during the study.

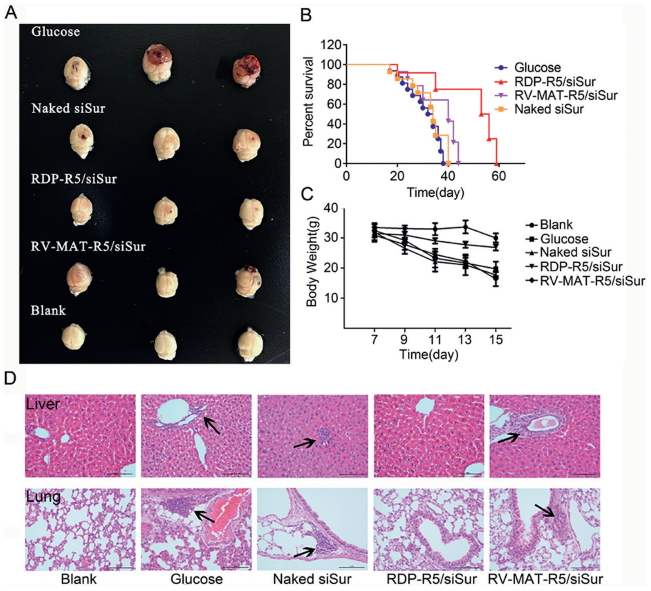

Fig. 5. (A) The representative photograph of excised tumors from treated mice with different formulations, blank refers to sham-operated group. (B) Percent survival of orthotopic glioma bearing mice in different groups. (C) Body weight of orthotopic glioma bearing mice in different groups ($n = 3$), blank refers to sham-operated group. Data are presented as mean ± SD. (D) H&E assay of liver and lung from treated mice with different formulations (blank arrows indicate metastasis loci), blank refers to sham-operated group, magnification 200×. Scale bar: 100 μm.

and RV-MAT-R5/siCy5 groups (Fig. S8B in Supporting information). However, siCy5 primarily accumulated in the excretory organ (kidney) in the RV-MAT-R5/siCy5 group, which may be attributed to poor brain accumulation and metabolism.

For non-tumor-bearing mice, after 1 h of administration, the brains were dissected and subjected to real-time *in vivo* fluorescence imaging. As shown in Fig. S9 (Supporting information), RDP-R5/siCy5 NPs had the significant fluorescence intensity in isolated brains of non-tumor bearing mice ($^{***}P < 0.001$). Almost no fluorescence was detected in isolated brains of naked siCy5 group and RV-MAT-R5/siCy5 NPs group. These results further indicated that RDP-R5/Cysi5 NPs possess superior BBB permeabilizing ability after intravenous injection.

The *in vivo* antitumor efficiency of RDP-R5/siSur was evaluated in orthotopic glioma models of ICR mice. As presented in Fig. 4, the luminescent signal intensity emanating from the tumors in all groups increased to different degrees within 16 days post-inoculation. On the 16th day after inoculation, the luminescent signal intensity in the brains of mice treated with glucose and naked siSur was high, and the tumor cells had infiltrated the surrounding regions. The tumors in the RV-MAT-R5/siSur group expanded slower than those in the glucose and naked siSur groups because of the enhanced permeability and retention (EPR) effect mediated by NPs [35,36]. Notably, the RDP-R5/siSur group demonstrated the best antitumor effect, attributed to the nAChR-mediated transcytosis strategy by RDP ligands for BBB penetration and enhanced glioma cell endocytosis. At the end of the experiment, the mice were cervically dislocated, and brain tissues were collected and photographed after washing the viscera with saline perfusion (Fig. 5A). Compared with normal brain tissues, brains in the glucose group displayed larger tumor volume, and glioma cells had infiltrated the brain with abundant angiogenesis and edema on the surface. In addition, the gliomas in the two negative control groups treated with naked siRNA and RV-MAT-R5/siSur NPs infiltrated the left hemisphere, with visible edema and hemorrhagic necrosis on the surface. In accordance with the luminescent signal assay, gliomas injected with RDP-R5/siSur NPs were relatively small in size and had less surface angiogenesis, suggesting that RDP-R5/siSur NPs inhibit growth and proximal tumor infiltration to some extent.

Terminal deoxynucleotidyl transferase dUTP nick end labeling (TUNEL) assay determines apoptotic cells in paraffin-embedded tissue sections, frozen tissue sections, cultured cells, and tissue-separated cells. For the purpose of explaining the tumor inhibitory effect from a cellular level perspective, gliomas were further investigated with TUNEL assays to analyze the biochemical and morphological characteristics of apoptotic cells. Representative images of each group are presented in Fig. S10 (Supporting information). Compared to other groups, mice treated with RDP-R5/siSur NPs exhibited a higher rate of glioma cell apoptosis (brown TUNEL-positive cells) in correlation with *in vivo* antitumor and *in vitro* apoptosis results. Notably, the apoptotic regions in the RDP-R5/siSur NPs group extended to the tumor interior, indicating that RDP could mediate sufficient tissue penetration of siRNA to suppress tumor cell vitality. However, a minute amount of RV-MAT-R5/siSur NPs reached the tumor tissue to induce apoptosis, with most of the apoptosis occurring at the edges of the tumor tissues. Therefore, in addition to the excellent BBB traverse potential, the enhanced tumor penetration of siRNA was another reason for the improved antitumor effect of RDP-R5/siSur NPs.

Liver and lung tissues were subjected to hematoxylin-eosin (H&E) staining to detect glioma metastasis. As presented in Fig. 5D, metastatic foci (black arrows) in the glucose, naked siSur, and RV-MAT-R5/siSur groups were observed in the liver and lung sections; however, no metastases were observed in the RDP-R5/siSur group, indicating that RDP-R5/siSur NPs inhibit the distant metastasis of tumors.

The body weight changes of the mice during administration are presented in Fig. 5C. The changes in body weight of treated mice reflect the progress of gliomas and the systemic toxicity of the administered formulations. Compared with the blank group, the body weight of mice in each group decreased over time, whereas that in the glucose, naked siSur, and RV-MAT-R5/siSur NPs groups decreased more rapidly. Mice treated with RDP-R5 or siSur NPs experienced slow weight loss. Therefore, RDP-R5/siSur NPs controlled disease progression and did not cause toxic side effects within the experimental dose range.

As presented in Fig. 5B, the survival rates of tumor-bearing mice in all the groups were investigated. The median survival time of tumor-bearing mice in both the glucose and naked siSur groups was 34 days, and 40 days in the RV-MAT-R5/siSur NPs group. In

particular, RDP-R5/siSur NPs prolonged the average survival time of tumor-bearing mice to 53 days. Compared with the naked siSur group and RV-MAT-R5/siSur group, the median survival time of mice in the RDP-R5/siSur NPs group was prolonged by 55.88% and 32.5%, respectively. Generally, the benefits of RDP-R5/siSur NPs in terms of prolonged survival time are attributed to the stability of siSur in the systemic circulation, effective BBB traverse and glioma cell endocytosis mediated by nAChR, sufficient glioma penetration, lower side effects, and exceptional inhibition of glioma growth and metastasis.

The safe and effective targeted delivery of therapeutic drugs into the brain is one of the most challenging fields in nano-drug delivery systems [37]. A polypeptide-carrier-mediated delivery system is the preferred option to address this problem. In this study, we developed a novel and effective polypeptide nanocarrier, RDP-R5, for siRNA delivery to gliomas. The RDP-R5/siRNA NPs exhibited stable and suitable physiochemical properties for *in vivo* applications and desirable glioma targeting efficiency and therapeutic efficacy. Moreover, the RDP-R5/siRNA NPs are easy to prepare, relatively stable in serum and possess good therapeutic effect on gliomas, which are promising for subsequent development and application in clinic. With the increasing prevalence of brain diseases (especially those lacking effective therapeutic approaches, such as Creutzfeldt-Jakob disease, neurodegenerative diseases, and brain tumors), RDP polypeptide nanocarriers-based brain-targeted siRNA delivery targeting disease-causing genes holds great promise for noninvasive, safe, and efficient treatment of various brain diseases.

Declaration of competing interest

The authors declare that they have no known competing financial interests or personal relationships that could have appeared to influence the work reported in this paper.

CRediT authorship contribution statement

Liqing Chen: Writing – original draft, Software, Methodology, Data curation. **Zheming Zhang:** Software, Methodology, Data curation. **Yanhong Liu:** Validation, Resources, Investigation. **Chenfei Liu:** Validation, Investigation, Formal analysis. **Congcong Xiao:** Software, Investigation, Data curation. **Liming Gong:** Resources, Investigation, Formal analysis. **Mingji Jin:** Supervision, Project administration, Formal analysis, Data curation. **Zhonggao Gao:** Writing – review & editing, Funding acquisition, Conceptualization. **Wei Huang:** Writing – review & editing, Funding acquisition, Conceptualization.

Acknowledgment

This work was supported by CAMS Innovation Fund for Medical Sciences (No. 2021-I2M-1-026, China).

Supplementary materials

Supplementary material associated with this article can be found, in the online version, at doi:10.1016/j.cclet.2024.110228.

References

[1] H. Yang, W. Li, Y. Xun, A.P. Yang, H. You, Mol. Ther. Oncolytics. 21 (2021) 1–14.
[2] Z.Y. Lin, R.W. Yang, K.S. Li, et al., BMC Neurol. 20 (2020) 310.
[3] T. Tykocki, M. Eltayeb, J. Clin. Neurosci. 54 (2018) 7–13.
[4] A. Aigner, D. Kögel, Nanomedicine 13 (2018) 89–103.
[5] C. Adida, P.L. Crotty, J. McGrath, D. Berrebi, J. Diebold, D.C. Altieri, Am. J. Pathol. 152 (1998) 43–49.
[6] G. Ambrosini, C. Adida, D.C. Altieri, Nat. Med. 3 (1997) 917–921.
[7] L.L. Kusner, M.J. Ciesielski, A. Marx, H.J. Kaminski, R.A. Fenstermaker, PLoS One 9 (2014) e102231.
[8] M. Zheng, W. Tao, Y. Zou, O.C. Farokhzad, B.Y. Shi, Trends Biotechnol. 36 (2018) 562–575.
[9] D. Karra, R. Dahm, J. Neurosci. 30 (2010) 6171–6177.
[10] J.M. Bergen, I.K. Park, P.J. Horner, S.H. Pun, Pharm Res. 25 (2008) 983–998.
[11] I. Mortimer, P. Tam, I. MacLachlan, et al., Gene Ther. 6 (1999) 403–411.
[12] Y.Y. Kuang, S. An, Y.B. Guo, et al., Int. J. Pharm. 454 (2013) 11–20.
[13] Y.Y. Kuang, X.T. Jiang, Y. Zhang, et al., Mol. Pharm. 13 (2016) 1599–1607.
[14] L. Wei, X.Y. Guo, T. Yang, et al., Int. J. Pharm. 510 (2016) 394–405.
[15] L. Wang, Y.W. Hao, H.X. Li, et al., J. Drug Target 23 (2015) 832–846.
[16] S. An, D.S. He, E. Wagner, C. Jiang, Small 11 (2015) 5142–5150.
[17] P. Kumar, H.Q. Wu, J.L. McBride, et al., Nature 448 (2007) 39–43.
[18] C. Gotti, F. Clementi, Prog. Neurobiol. 74 (2004) 363–396.
[19] M.K. Qu, Q. Lin, S.S. He, et al., J. Control. Release 277 (2018) 173–182.
[20] Y. Han, C.H. Gao, H. Wang, et al., Bioact. Mater. 6 (2021) 529–542.
[21] C.Q. Qiao, R.L. Zhang, Y.D. Wang, et al., Angew. Chem. Int. Ed. 59 (2020) 16982–16988.
[22] S.B. Ruan, Y. Zhou, X.G. Jiang, H.L. Gao, Adv. Sci. 8 (2021) 2004025.
[23] J.L. Yang, X.F. Zhang, X.J. Chen, L. Wang, G.D. Yang, Mol. Ther. Nucleic Acids 7 (2017) 278–287.
[24] J.M. Cooper, P.B. Wiklander, J.Z. Nordin, et al., Mov. Disord. 29 (2014) 1476–1485.
[25] J.W. Cui, Y.X. Xu, H.Y. Tu, et al., Acta Pharm. Sin. B 12 (2022) 1100–1125.
[26] T.I. Terpinskaya, A.V. Osipov, E.V. Kryukova, et al., Mar. Drugs 19 (2021) 118.
[27] S. Danthi, R.T. Boyd, Neurosci. Lett. 400 (2006) 63–68.
[28] C. Thongbamrer, W. Roobsoong, J. Sattabongkot, P. Opanasopit, B.E. Yingyongnarongkul, ChemBioChem 23 (2022) e202100672.
[29] F. Li, N.C. Song, Y.H. Dong, et al., Angew. Chem. Int. Ed. 61 (2022) e202116569.
[30] S. Salatin, S. Maleki Dizaj, A. Yari Khosroushahi, Cell. Biol. Int. 39 (2015) 881–890.
[31] X.T. Qi, J.S. Zhan, L.M. Xiao, et al., Neurochem. Res. 42 (2017) 1847–1863.
[32] C.D. Arvanitis, G.B. Ferraro, R.K. Jain, Nat. Rev. Cancer 20 (2020) 26–41.
[33] L. Chen, D. Zeng, N. Xu, et al., ACS Appl. Mater. Interfaces 11 (2019) 41889–41897.
[34] D. Janigro, S.M. Leaman, K.A. Stanness, Pharm. Sci. Technol. Today 2 (1999) 7–12.
[35] M.A. Subhan, S.S.K. Yalamarty, N. Filipczak, F. Parveen, V.P. Torchilin, J. Pers. Med. 11 (2021) 571.
[36] R. Liu, C. Luo, Z. Pang, et al., Chin. Chem. Lett. 34 (2023) 107518.
[37] H. Wu, Y.M. Wang, Z.K. Ren, et al., Chin. Chem. Lett. (2024), doi:10.1016/j.cclet.2024.109996.